T-lymphoblastic lymphoma in a child diagnosed by metagenomic sequencing: A case report

LIANQIN MO[1], JUN JIANG[1], JUAN SHI[1], ZEMIN YU[2], LINGYI LI[2] and DONG HUANG[1]

[1]Department of Pediatric Intensive Care, Guizhou Provincial People's Hospital, Guiyang, Guizhou 550002; [2]Department of Medicine, Hangzhou Matridx Biotechnology Co., Ltd., Hangzhou, Zhejiang 311112, P.R. China

Received January 5, 2023; Accepted April 28, 2023

DOI: 10.3892/ol.2023.13875

Abstract. T-lymphoblastic lymphoma (T-LBL) is a rare subtype of non-Hodgkin's lymphoma with a higher incidence in children than adults. T-LBL often presents with multiple lymph node enlargements or mediastinal masses, which can cause local compression symptoms, and is frequently misdiagnosed as an infectious disease at an early stage. By summarizing a recently experienced case of T-LBL in a patient with a suspected infection, with an analysis of clinical features and diagnostic methods, the aim of the present study was to provide more information on the early diagnosis of tumors in patients suspected to have an infection. An 8-year-old boy presented at a local hospital with abdominal pain, chest tightness and shortness of breath for >5 days, and bilateral pleural, abdominal and pericardial effusion were considered. Following hospitalization without significant improvement under treatment with an anti-infection regimen and closed chest cavity drainage, the patient was transferred to another hospital. Once admitted, ultrasound examination indicated a large amount of pericardial and pleural effusion. Pericardiocentesis and closed chest cavity drainage were performed immediately. The initial pericardial drainage, which was bloody in appearance, gradually changed to a pale-yellow fluid. The patient continued to present with a temperature and remained under active anti-infection treatment. With repeated drainage procedures, it was observed that the volume of fluid obtained from the closed chest cavity exhibited an increasing trend. The cytological and tumor marker analysis of the idiopathic effusion specimens detected no abnormalities. Metagenomic next-generation sequencing (mNGS) of the pericardial drainage fluid was performed to identify the infectious pathogen. No pathogen was detected in the specimens, but the copy number variation (CNV) found in multiple chromosomes was highly suggestive of cancer development and progression. Lung imaging revealed no mediastinal lesions or tumors. The fluid from a subsequent closed chest drainage procedure was evaluated by mNGS for diagnostic purposes, and multiple CNVs were again noted, with similar results to those from the pericardial effusion. To determine the tumor type, immunophenotyping of the fluid was performed using flow cytometry and a diagnosis of T-LBL was confirmed. The patient was subsequently transferred to the hematology department for chemotherapy. The present case indicates that mNGS can not only differentiate between infections and tumors but also rapidly determine disease etiology.

Correspondence to: Ms. Lingyi Li, Department of Medicine, Hangzhou Matridx Biotechnology Co., Ltd., 2073 Jinchang Road, Yuhang, Hangzhou, Zhejiang 311112, P.R. China
E-mail: 001lly@sina.com

Professor Dong Huang, Department of Pediatric Intensive Care, Guizhou Provincial People's Hospital, 83 Zhongshan Dong Road, Nanming, Guiyang, Guizhou 550002, P.R. China
E-mail: hd522523@163.com

Key words: T-lymphoblastic lymphoma, non-Hodgkin's lymphoma, copy number variation, metagenomic next-generation sequencing, multiple serous cavity effusion

Introduction

T-lymphoblastic lymphoma (T-LBL) is a rare subtype of non-Hodgkin lymphoma (NHL), accounting for ~2% of all cases of NHL (1-4). T-LBL has a high incidence in children, in which it constitutes approximately one-third of NHL cases; it is also more prevalent in men than in women, and is typically a highly aggressive lymphoma with extremely poor therapeutic efficacy. It advances rapidly, is characterized by extensive lesions and is often accompanied by mediastinal masses and central nervous system (CNS) infiltration. Patients with T-LBL predominantly present with multiple lymph node involvement or mediastinal masses, but rarely exhibit bone marrow invasion. Local compression symptoms may occur and are often associated with tumor cells originating from the thymus. The disease may also invade the pleura and pericardium, causing serous cavity effusion.

Metagenomic next-generation sequencing (mNGS) can be used for the unbiased sequencing of human and microbial nucleic acids in clinical specimens. It has the advantages of being a hypothesis-free diagnostic approach, requiring no culturing and having a short turn-around time. It has been widely used in the diagnosis and treatment of infectious diseases, and its sensitivity is significantly higher than that of the traditional culture method (61.0% vs. 19.5%) (5). The metagenomic sequencing of body fluids has enabled previously

undiagnosed tumors to be identified via the detection of human chromosome copy number variations (CNVs), and may facilitate the early diagnosis of tumors and promote the timely and evidence-based treatment of patients (6).

The present case report describes a case of abdominal pain, chest tightness and shortness of breath in an 8-year-old boy. When the patient was admitted following multiple serous cavity effusions, the imaging and clinical presentation and routine blood biochemistry were similar those seen in infectious diseases such as tuberculosis, leading to a delayed diagnosis. However, a diagnosis was ultimately made based on analysis of the serous cavity fluid using mNGS. The test excluded microbial infection while simultaneously detecting chromosomal abnormalities that conformed to the chromosomal characteristics of a malignant neoplasm. Flow cytometric immunophenotyping of the pleural effusion revealed that the neoplasm was T-LBL.

Case report

In August 2022, an 8-year-old male child was admitted to Huishui County Lianjiang Hospital having experienced abdominal pain for 6 days accompanied by chest tightness and shortness of breath for >5 days. Chest digital radiography and computed tomography (CT) were performed in the local hospital, which indicated a large amount of left pleural effusion, compression atelectasis and pericardial effusion in the left lung. The patient was treated with an anti-infection regimen and a closed chest drainage procedure following local hospitalization. Following recurrence of the left pleural effusion, the patient was transferred to Guizhou Provincial People's Hospital (Guiyang, China) 3 days later. Physical examination revealed rapid breathing, an increased heart rate, the inability to lie supine, jugular vein irritation, a positive hepatic jugular vein reflux sign, unobstructed left chest drainage, and bloody and turbid effusion. The thorax was normal, without sternal percussion pain or a subcutaneous twisting sensation when touched; however, slight widening of the left intercostal space was observed. The respiratory activity of the left lower lung was diminished and the speech pattern of the patient was weak and irregular. In addition, the percussive sound of the left lung was tympanic and its breathing sound was significantly deeper than that of the right lung, which exhibited a light percussive tone and deep breathing sound. Low-pitched and distant heart sounds in the chest were heard through a stethoscope. The ribs displayed no tenderness upon palpation. The clinicians suggested that pericardiocentesis should be performed immediately after cardiac tamponade; therefore, the left closed chest drainage system was preserved. The main laboratory findings are shown in Tables I and II.

Following admission, the child had a recurrent fever with a highest recorded temperature of 38.9˚C. Blood CRP was elevated and the white blood cell count was higher than the normal range.. Routine blood tests indicated that the percentage of neutrophils was elevated. The pericardial and pleural effusion was identified as an exudate. A high-resolution CT scan of the lungs (Fig. 1A) revealed multiple exudation sites and inflammation in both lungs. This was more severe in the left lung, with partial compression and expansion of the left lower lobe, left main bronchial stenosis, blurred mediastinal borders and a large amount of fluid accumulated in the pericardium (Fig. 1B). This was attributed to severe necrotizing pneumonia with the possibility of infectious disease.

Initial treatment. After admission, the left closed chest drainage system was retained and remained unobstructed. Due to signs of a large amount of pericardial effusion, pericardiocentesis was performed and immediately followed by ultrasound monitoring. Pleural reaction and heart failure occurred during the puncture, and the patient was endotracheally intubated for mechanical ventilation. Anti-infection treatment was cefoperazone sulbactam (75 mg/kg/dose via intravenous infusion pump once every 8 h) combined with azithromycin (10 mg/kg/dose via intravenous infusion pump once daily). Anti-inflammatory treatment was performed with methylprednisolone sodium succinate (1-2 mg/kg/dose), milrinone (0.5 μg/kg/min) and dobutamine (5 μg/kg/min) for cardiac stimulation. Myocardial nutrition was administered using sodium fructose diphosphate. After these treatments, no fever was observed and the abdominal pain, chest pain and shortness of breath were markedly ameliorated. The endotracheal intubation and ventilator were successfully withdrawn and the patient was able to breathe stably using a nasal catheter. After 11 days of treatment, the volume of pericardial drainage fluid gradually decreased and the color of the fluid changed from bloody to pale yellow. The condition of the patient improved following the anti-infection treatment, which supported the diagnosis of an infectious disease. However, the fluid volume obtained by closed-chest drainage was not notably reduced, the daily diverted flow increased (200-350 ml), and the color of the fluid changed from bloody to light yellow.

mNGS testing. The routine diagnostic tests were negative after admission. However, large volumes of pericardial and pleural effusions continued to be generated following the anti-infection treatment. To clarify the cause of this, pericardial drainage fluid was collected for mNGS testing and no pathogens were detected. However, mNGS was also used perform a CNV analysis of the host chromosome (Data S1). Following normalization of the data and comparison with data from a healthy individual with no known genetic disease, abnormalities (duplications and deletions) were identified in chromosomes 1, 6, 9, 12, 16, 17 and 19. The deletion of large segments (>10 megabase pairs), which may have occurred due to chromosomal instability, suggested that the patient may have a tumor. The temperature of the patient was normal, and although the volume of pericardial fluid drainage gradually decreased following anti-infection treatment, the volume of thoracic drainage fluid remained copious. Magnetic resonance imaging (MRI) examination of the mediastinum indicated that the thymus was enlarged and its signal was not uniform. Due to the pleural and pericardial effusion, the left pleura appeared to be slightly thickened, and no obvious space-occupying lesions were observed. To further investigate the cause of the pleural effusion, mNGS was applied to the pleural drainage fluid. The results revealed the presence of *Escherichia coli* (sequence reads, 19; relative abundance, 11.18%). The CNV analysis of the pleural drainage also revealed abnormalities, with chromosomal variant sites similar to those found in the pericardial drainage fluid (Fig. 2). Notably, numerous expansions and

Table I. Examinations during hospitalization.

	Number of days after hospitalization												
Tests[a]	1	2	3	4	5	6	7	8	9	10	11	12	13
Routine blood tests													
WBC (x10^9)	14.34	12.4	-	-	-	15.66	-	-	13.14	-	-	-	-
N%	67.6	62.8	-	-	-	77.4	-	-	61.7	-	-	-	-
Blood biochemistry													
CRP (mg/l)	46.41	17.96	14.23	-	-	2.62	-	-	0.68	-	-	-	-
PCT (ng/ml)	-	0.21	0.2	-	-	-	-	-	-	-	-	-	-
Lactate dehydrogenase (U/l)	604	589	387	-	-	399	-	-	333	-	-	-	-
Uric acid (μmol/l)	500	331	-	-	-	151	-	-	160	-	-	-	-
α-hydroxybutyrate dehydrogenase (U/l)	525	466	329	-	-	324	-	-	260	-	-	-	-
Blood tumor markers													
NSE (μg/l)	-	-	35	-	-	-	-	-	-	24.1	-	-	-
CA125 (U/ml)	-	-	161	-	-	-	-	-	-	104	-	-	-
Serous cavity edema													
Thoracic closed drain (ml)	No	No	200, light blood	No	No	250, blood	350, blood	200, bloody	125, yellow	200, light yellow	50, light yellow	225, light yellow	275, light yellow
Pericardial drainage (ml)	No	No	145, blood	270, blood	205, blood	70, blood	75, bloody	60, bloody	40, yellow	20, light yellow	30, light yellow	No	No
Effusion, routine and biochemical[b]													
Pigment	-	Red	-	-	-	Red	-	-	-	-	-	-	-
Clearness	-	Cloudy	-	-	-	Lightly cloudy	-	-	-	-	-	-	-
Mucin	-	Positive	-	-	-	Positive	-	-	-	-	-	-	-
TCS (x10^6/l)	-	58,250	-	-	-	63,600	-	-	-	-	-	-	-
ADA (U/l)	-	153	-	-	-	24.1	-	-	-	-	-	-	-
Chlorine (mmol/l)	-	109.1	-	-	-	111.3	-	-	-	-	-	-	-
Glucose (mmol/l)	-	5.75	-	-	-	8.34	-	-	-	-	-	-	-
Lactate dehydrogenase (U/l)	-	873	-	-	-	312	-	-	-	-	-	-	-
Etiology													
Eaton's reagent	-	1:80+	-	-	-	-	-	-	-	-	1:160+	-	-
Maximum temperature (˚C)	36.7	36.3	38.6	38.9	36.7	36.8	36.9	36.8	36.9	38.7	36.9	36.8	36.9
Maximum heart rate (beats/min)	133	124	157	151	124	134	98	89	93	89	94	85	85

[a]Normal reference values: WBC, 4.3-11.3x10^9/l; N%, 31-70%; CRP, 0-5 mg/l; PCT, 0-0.07 ng/ml; lactate dehydrogenase, 110-295 U/l; uric acid, 210-420 μmmol/l; α-hydroxybutyric dehydrogenase, 53-168 U/l; ADA 0-35U/l; NSE, 0-16.3 μg/l; CA125, 0-35 U/ml; serous cavity edema, chlorine 99-110 mmol/l; amylase, the leakage fluid was consistent with the blood sugar, and the sugar content in the exudate was reduced or eliminated; lactate dehydrogenase in the leakage fluid <200 U/l. [b]Results on the first day of admission are for pericardial effusion and on the fifth day of hospital admission are for pleural effusion. WBC, white blood cell; N%, neutrophil percentage; CRP, C-reactive protein; PCT, procalcitonin; NSE, neuron-specific enolase; CA125, cancer antigen 125; TCS, total cell solids; ADA, adenosine deaminase.

deletions were detected among the CNVs in chromosome 9, which indicated the presence of tumor DNA in this body fluid. It must be noted that the variation sites in the two types of drainage fluid were not exactly the same. This is likely due to tumor nucleic acid fragments varying in different body fluids; in general, the closer the fluid is to the lesion, the higher the concentration of tumor nucleic acid fragments (7). Therefore, it was inferred that the tumor was located in the mediastinum.

Table II. General results.

Examinations	Findings
Blood biochemistry	Blood ammonia, blood lactate and B-type natriuretic peptide negative; renal function, coagulation function, electrolytes, blood glucose, liver function and myocardial enzyme normal
Blood tumor markers	Carbohydrate antigen 19-9, α-fetoprotein, carcinoembryonic antigen and ferrotin normal
Etiology	Three tuberculosis tests, T-SPOT, resist O, respiratory pathogen tests (A and B influenza virus, adenovirus, respiratory syncytial virus, mycoplasma and rhinovirus), Epstein-Barr virus antibody and DNA tests, preoperative infectious diseases screen, pericardial effusion smear and culture, pleural effusion smears and the culture all negative
Rheumatic immunity and connective tissue	Thyroid function, complement C3 and C4, rheumatoid factor, erythrocyte sedimentation rate, lymphocyte immunity somatotype and anti-neutrophil cytoplasmic antibodies all negative. Antinuclear antibody profiles for anti-nRNP/Sm and anti-Sm weakly positive
Imaging	High resolution lung CT revealed inflammation and exudate in both lungs, although mainly in the left lung, and regional compression, expansion and pulmonary insufficiency after drainage of the left pleural effusion; left main bronchus stenosis; blurred fat space and unclear layers in the mediastinum; large accumulation of pericardial effusion. Abdominal CT revealed no obvious abnormality
Heart ultrasound	Large amount of pericardial effusion. Left ventricular systolic function measurement normal

CT, computed tomography; Sm, Smith; nRNP, nuclear ribonucleoprotein.

Follow-up and outcomes. After admission, testing for autoantibodies revealed no abnormalities. No cancer cells were observed during the cytological examination of the pericardial drainage fluid (Fig. 3A) and thoracic drainage fluid (Fig. 3B). Furthermore, cytomorphological examination revealed no abnormal cell hyperplasia in the bone marrow. Flow cytology immunophenotyping of the pleural effusion was performed (Data S1). Gated on the CD45/side scatter dot plot, the abnormal cell population was visible in the original cell distribution area, comprising ~58% of the nuclear cells, which were positive for the expression of CD3, CD4, CD5, CD7, CD10, CD38, CD58, T-cell receptor γ/δ, cytoplasmic CD3 and terminal deoxynucleotidyl transferase. No juvenile lymphocytes were detected in the peripheral blood. Myeloid proliferation was observed to be significantly inhibited. According to the World Health Organization National Comprehensive Cancer Network (NCCN) Clinical Practice Guidelines for Oncology (second edition, 2015) (8), the patient's flow cytometric results were consistent with a T-LBL immunophenotype (Fig. 3C). The patient was diagnosed with acute T-LBL with intermediate risk and transferred to the pediatric hematology department for further specialist treatment. Following transfer, pre-chemotherapy examinations were conducted and the treatment plan was determined. This was communicated to the patient's family, who provided informed consent. The treatment strategy adopted was in accordance with the guidelines for the intermediate-risk disease as described in the Pediatric Acute Lymphoblastic Leukemia Diagnosis and Treatment Guidelines (2020 edition) (9). It included the CVDLD regimen, comprising prednisone, dexamethasone, vindesine, daunorubicin, cyclophosphamide and intramuscular pemaspartase as follows: prednisone tablets (60 mg/m^2/day orally on days 1-7); dexamethasone (6-8 mg/m^2/day orally or intravenously on days 8-28, reduced for 7 days); vindesine (3 mg/m^2/day intravenously on days 8, 15, 22 and 29); daunorubicin (30 mg/m^2/day for 1 h on days 8, 15, 22 and 29; cyclophosphamide (1 g/m^2 by intravenous drip on day 8); and intramuscular pemaspartase injection (2,500 U/m^2/day on days 9 and 23, twice in total). Remission was observed. Evaluation of the bone marrow cells revealed that on day 15 of the CVDLD-induced remission, the cell morphology was M1, but the bone marrow minimal residual disease (MRD) was <3.4%, leading to an adjustment of the risk group to high risk. By day 33 of CVDLD treatment, the morphology of bone marrow cells exhibited a complete response, and the bone marrow MRD was <0.01%. The patient continued to be evaluated, and eventually achieved a complete response following two rounds of early intensive therapy with CAML (10) [Cytoxan, 750-1000 mg/m^2/day, once a day, intravenously; cytosine arabinoside, 75-100 mg/m^2/day, for 7-8 days, 1-2 times a day, intravenously; 6-mercaptopurine, 50-75 mg/m^2/day, for 7-14 days, orally on an empty stomach. Pegaspargase (CAML regimen) 2,000-2,500 U/m^2/day, on day 2, once, intramuscularly; or home DXM on top of CAML 8 mg/m^2/day orally, days 1-7]. Next, the child began the consolidation protocol according to treatment guidelines.

Discussion

The present report describes a pediatric patient with T-LBL who presented with abdominal pain, chest tightness and shortness of breath and was initially diagnosed with multiple serous effusions. Laboratory tests and imaging findings, including negative results for tumor markers and serous effusion cells, normal blood tests and response to repeated anti-infection treatment indicated an infection. However, multiple CNVs in the host chromosome were detected by mNGS, suggesting the possibility of a tumor. Flow cytological immunotyping

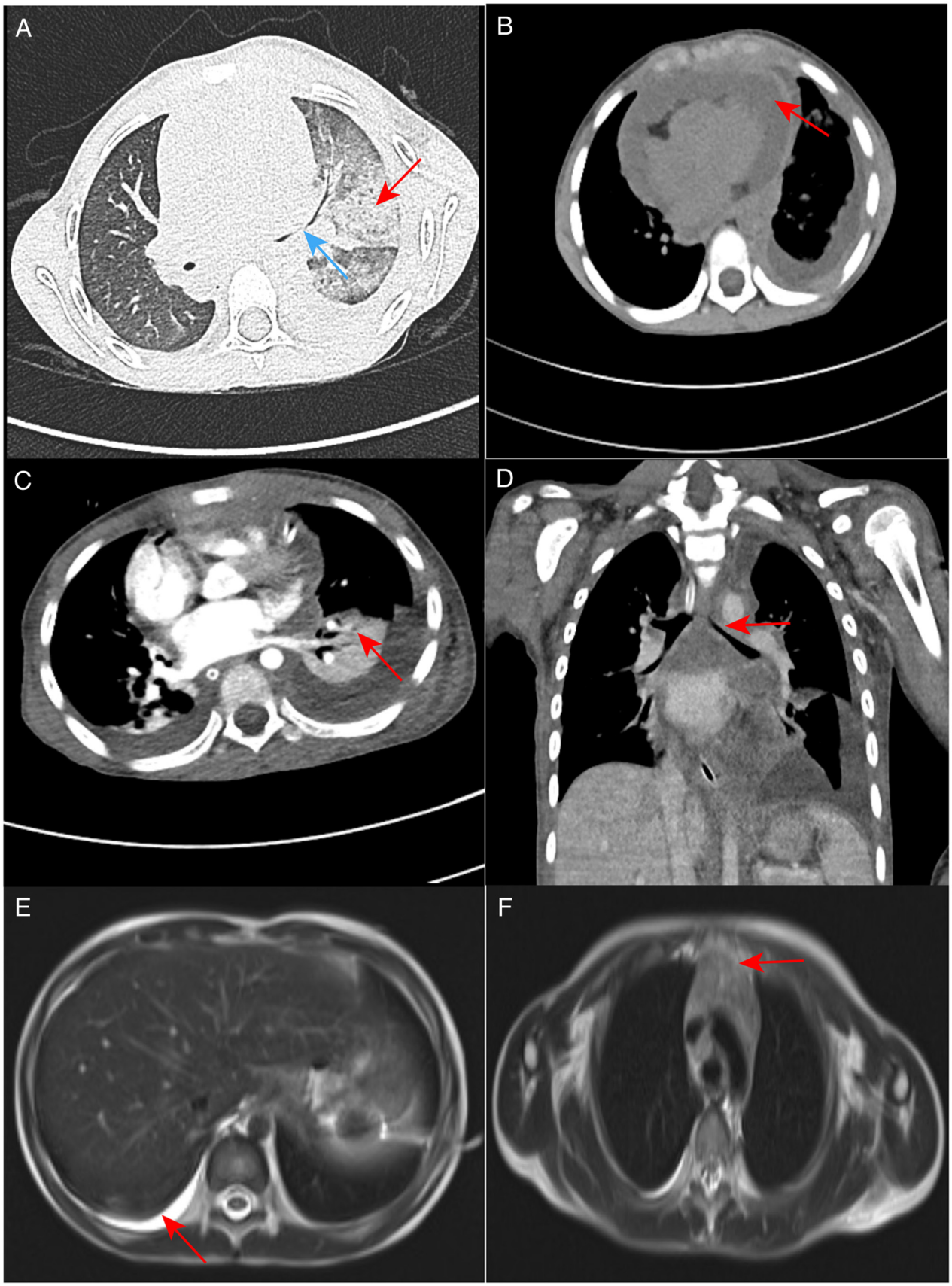

Figure 1. CT and MRI images of the patient. (A) High-resolution CT scan of the lungs in August 2022. Multiple areas of inflammation and exudation in both lungs are shown, with increased severity in the left lung (red arrow), left pleural effusion drainage, partial left lower lobe compression and expansion, and stenosis of the left main bronchus (blue arrow). (B) High-resolution CT scan of the lungs in August 2022; the mediastinal fat space appears blurred and indistinct, and the accumulation of a large amount of fluid is visible in the pericardium (red arrow). (C) Enhanced CT scans of the lungs in August 2022 show marked solidity in the left lung (red arrow) and (D) left main bronchial stenosis (red arrow). (E) In September 2022, an enhanced MRI scan of the mediastinum revealed significant pleural effusion on the right side (red arrow). (F) The thymus was enlarged (red arrow). CT, computed tomography; MRI, magnetic resonance imaging.

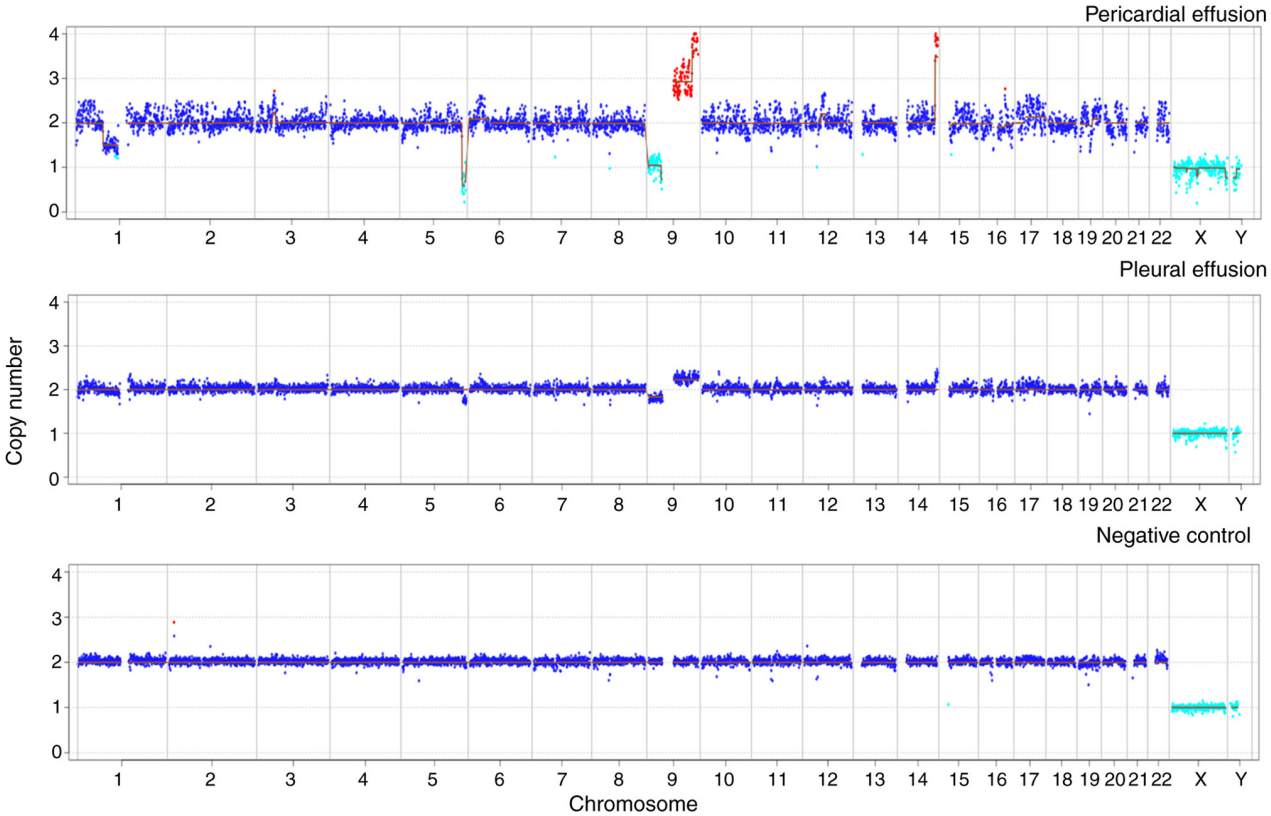

Figure 2. Chromosome copy number variation analysis in patient samples. The pericardial and pleural effusion samples for the present case showed increased and absent chromosome copy numbers on a large segment of chromosome 9. The negative control was pleural effusion from an individual with no known genetic disease.

of the pleural effusion finally confirmed the diagnosis of T-ALL/LBL. T-cell lymphomas mainly present as LBL with a small number presenting as ALL. T-ALL/LBL commonly affects older children, with a median onset age of 9-12 years. Clinical symptoms include an anterior mediastinal mass, airway compression symptoms, dysphagia and venous obstruction. Lymph node lesions are common, particularly in the neck, supraclavicular and axilla regions, while ~50% of cases have bone marrow involvement. CNS metastases occur in ~15% of cases, with meningeal lesions occurring more frequently than parenchymal lesions (11).

Multiple serous body cavity effusion is a frequently occurring disease, which comprises the simultaneous presence of effusion in two or more of the serosal cavities, which comprise the pericardial, thoracic and abdominal cavities. Due to the complex etiology of multiple serous body cavity effusions and the heterogeneous clinical manifestations, diagnosis is challenging. Moreover, the differentiation of malignant and nonmalignant effusions is important for the subsequent treatment and prognostic evaluation of this disease. Multiple serous body cavity effusion can occur as an isolated disease or in association with a wide spectrum of systemic diseases. A previous study conducted an etiological analysis of 241 patients with multiple serous body cavity effusions, of which 11.6% had an unknown etiology (12). The most common cause of these effusions in patients with clear etiology was malignancy (32.8%), followed by autoimmune diseases (13.3%), tuberculosis (8.3%), cirrhosis (7.9%) and cardiac insufficiency (6.2%). In another study in which 92 patients with multiple serous body cavity effusions were analyzed, 38% of cases had unknown etiology, and the most common diagnosis in patients with clear etiology was malignancy (30.4%), followed by infectious diseases (15.2%) and autoimmune diseases (13.0%) (13).

In the relevant auxiliary examination of the present case, the results of autoimmunity-associated tests were negative and did not support an autoimmune disease. Etiological examination revealed that the adenosine deaminase (ADA) levels in the pericardial effusion were markedly increased, and the measurement of ADA activity in serous cavity effusions has been shown to have high specificity and sensitivity in the diagnosis of tuberculous infection (14). However, in the present case the ADA levels in the pleural effusion were normal, and the results of tuberculosis and T-SPOT. TB assays were normal. These negative results did not support the involvement of tuberculosis. The mNGS sequencing results for the pleural effusion suggested that a nosocomial *Escherichia coli* infection must be considered. The blood mycoplasma antibody titer of the child was elevated (1:160), but his mycoplasma nucleic acid test was negative and therefore not supportive of a recent infection. The negative pathogen detection results did not support an infectious disease as the cause of the effusions. No secondary or tertiary blood reduction was evident and no original naive T cells were detected. The carbohydrate antigen 19-9, α-fetoprotein, carcinoembryonic antigen and ferritin results were normal. The chest CT scan and enhancement did not reveal any space-occupying lesions. Mediastinal MRI scan and enhancement also did not indicate any organic lesions, but instead suggested enlargement of the mediastinum and small hilum lymph nodes. T-LBL is

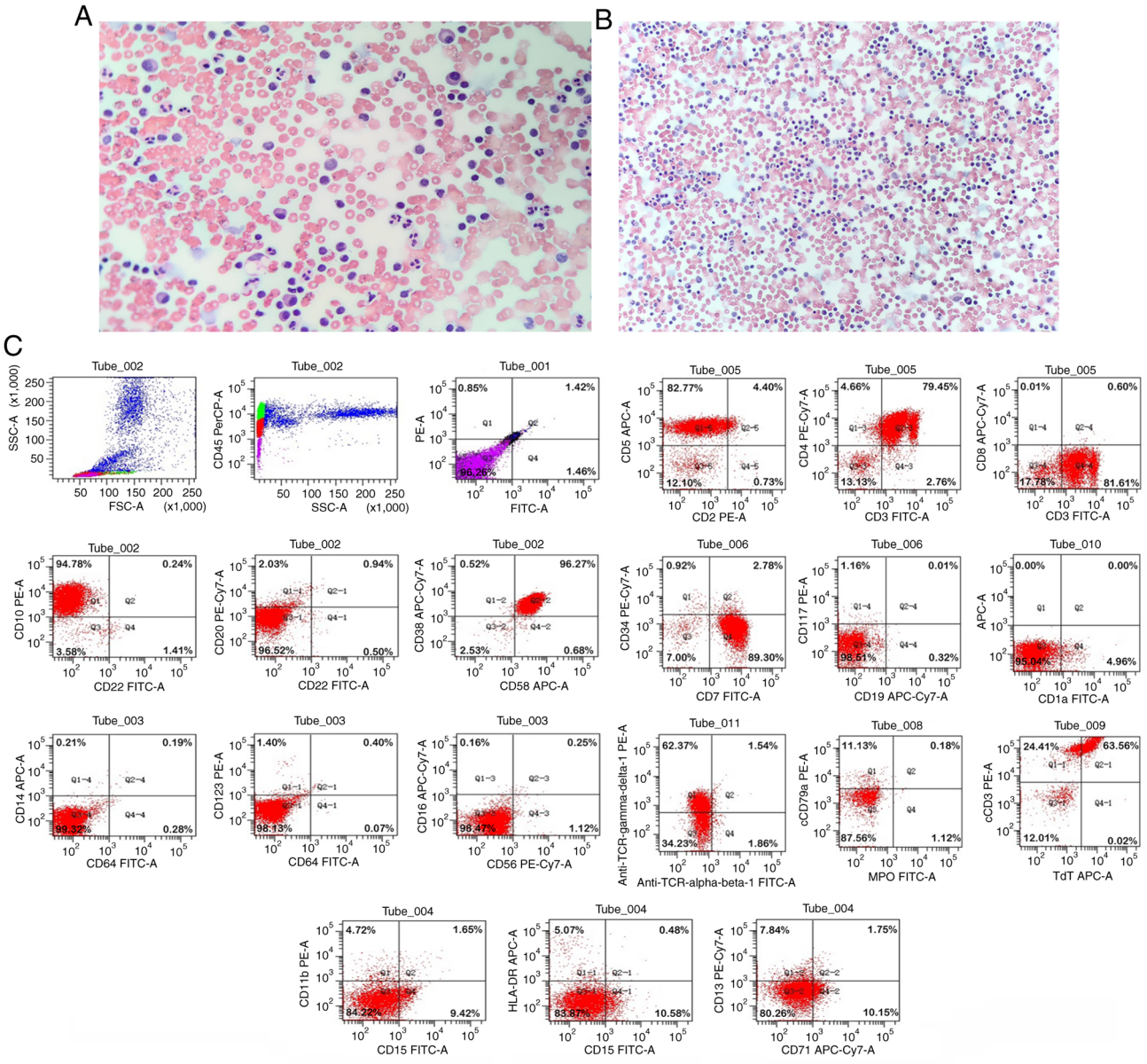

Figure 3. Papanicolaou staining and flow cytometry results for the present case. Papanicolaou staining revealed no heterotypic cells in the (A) pericardial drainage fluid (magnification, x200) and (B) thoracic drainage fluid (magnification, x100). (C) Gate analysis on the CD45/SSC dot plot showed an abnormal cell population in the original cell distribution region, comprising ~58% of the nuclear cells, with positive expression of CD3, CD4, CD5, CD7, CD10, CD38, CD58, TCR γ/δ, cCD3 and TdT. Myeloid proliferation was significantly inhibited. SSC, side scatter; TCR, T-cell receptor; cCD3, cytoplasmic CD3; TdT, terminal deoxynucleotidyl transferase.

known to present a mediastinal mass in 60-70% of cases, often with shortness of breath, due to superior vena cava compression or pericardial and/or pleural effusion (15). Tests and procedures used to diagnose T-cell blastic lymphoma include bone marrow biopsy, immunohistochemistry, flow cytometry, polymerase chain reaction testing and the fluorescence *in situ* hybridization testing of major chromosomal translocations. Furthermore, in certain cases, MRI and positron emission tomography-CT can facilitate the diagnostic examination. In the diagnosis and treatment of the present child, based on the rarity of T-LBL, the nonspecific diagnosis of malignancy by the cytological examination of multiple serous body cavity effusions, and the low positivity rate of carcinoembryonic antigen, numerous tests did not support the diagnosis of cancer, which easily resulted in a misdiagnosis.

mNGS has been used increasingly widely in the clinic in recent years, and has gradually emerged as an important method for the detection of pathogens in infectious diseases. When pathogenic microorganisms are detected in a patient sample, a large number of host nucleic acids are also present; therefore, the host nucleic acid must be filtered. A number of studies have assisted in the diagnosis of lymphoma (16), meningeal carcinoma (17) and squamous cell lung carcinoma (18) via the analysis of CNVs in the host chromosome. Cancer cells are characterized by structural variation during division, as chromosomal instability is common in tumors (19). A CNV is a change in the copy number of one or more genes, and CNVs are an important component of the genetic variation involved in the development of multiple types of cancers. CNVs are present in ~90% of solid tumors (20), but the sensitivity for their detection

is low (21). CNVs caused by tumors appear as duplications or deletions of large fragments or entire chromosomes, so the large CNVs (>10 M) encompassing several chromosomes were unlikely to be false-positives (6). In the present case, several host chromosomes in the pericardial effusion were found to contain abnormalities, although in lower quantities than would be expected in a patient with congenital chromosomal abnormalities (18). This allowed a diagnosis of genetic chromosomal changes to be excluded. The chromosomal examination of multiple serous cavity effusions is considered to be beneficial for the diagnosis of benign and malignant diseases (22). mNGS is able to detect many types of pathogens in one test, including low levels of pathogens, and is useful for detecting coinfections (23). However, it also presents false positives and can be difficult to interpret. It is also expensive.

As a novel method for the clinical detection of infectious pathogens, mNGS can analyze human CNVs or aneuploidy in addition to providing data on pathogenic microbes. Even though the detection of chromosomal CNVs using mNGS cannot provide a definitive cancer diagnosis, following the exclusion of infection it can provide an early warning of a clinical tumor diagnosis and improve the likelihood of tumor detection. In the present study, mNGS performed on human body fluids suggested the presence of a tumor. It may serve as a reference case for the analysis of pathogens and chromosomal CNVs in the detection of pediatric T-LBL.

Acknowledgements

Not applicable.

Funding

No funding was received.

Availability of data and materials

The datasets used and/or analyzed during the current study are available in the Sequence Read Archive [https://www.ncbi.nlm.nih.gov/sra/?term=PRJNA901203].

Authors' contributions

LQM is the primary physician who performed the diagnosis and treatment of the patient. JJ and JS collected and analyzed clinical and sequencing data. ZMY processed images, and collected and collated data. LQM, DH and LYL wrote the manuscript. DH and LYL conceived and designed the study. LQM, DH and LLY confirm the authenticity of all the raw data. All authors have read and approved the final version of the manuscript.

Ethics approval and consent to participate

Not applicable.

Patient consent for publication

Written informed consent was obtained from the legal guardian of the patient for the publication of any potentially identifiable images or data in this article.

Competing interests

LYL and ZMY are employees of Hangzhou Matridx Biotechnology Co., Ltd. The other authors declare that they have no competing interests.

References

1. Cortelazzo S, Ponzoni M, Ferreri AJ and Hoelzer D: Lymphoblastic lymphoma. Crit Rev Oncol Hematol 79: 330-343, 2011.
2. Park HS, McIntosh L, Braschi-Amirfarzan M, Shinagare AB and Krajewski KM: T-cell non-hodgkin lymphomas: spectrum of disease and the role of imaging in the management of common subtypes. Korean J Radiol 18: 71-83, 2017.
3. Swerdlow SH, Campo E, Pileri SA, Harris NL, Stein H, Siebert R, Advani R, Ghielmini M, Salles GA, Zelenetz AD and Jaffe ES: The 2016 revision of the World Health Organization classification of lymphoid neoplasms. Blood 127: 2375-2390, 2016.
4. Vose J, Armitage J and Weisenburger D: International peripheral T-cell and natural killer/T-cell lymphoma study: Pathology findings and clinical outcomes. J Clin Oncol 26: 4124-4130, 2008.
5. Hogan CA, Yang S, Garner OB, Green DA, Gomez CA, Dien Bard J, Pinsky BA and Banaei N: Clinical impact of metagenomic next-generation sequencing of plasma cell-free DNA for the diagnosis of infectious diseases: A multicenter retrospective cohort study. Clin Infect Dis 72: 239-245, 2021.
6. Gu W, Talevich E, Hsu E, Qi Z, Urisman A, Federman S, Gopez A, Arevalo S, Gottschall M, Liao L, *et al*: Detection of cryptogenic malignancies from metagenomic whole genome sequencing of body fluids. Genome Med 13: 98, 2021.
7. Tivey A, Church M, Rothwell D, Dive C and Cook N: Circulating tumour DNA-looking beyond the blood. Nat Rev Clin Oncol 19: 600-612, 2022.
8. Alvarnas JC, Brown PA, Aoun P, Ballen KK, Barta SK, Borate U, Boyer MW, Burke PW, Cassaday R, Castro JE, et al: Acute Lymphoblastic Leukemia, Version 2.2015. J Natl Compr Canc Netw 13: 1240-1279, 2015.
9. Tianyou Wang XS, Zhang Y, Tang J, Jin L, Yang J, Duan Y, Zhou C, Gao Z and Qu X: Childhood lymphoblastic lymphoma treatment standard (2019 update). National Health Commission of the PRC 716: 10-29, 2019 (In Chinese).
10. Koprivnikar J, McCloskey J and Faderl S: Safety, efficacy, and clinical utility of asparaginase in the treatment of adult patients with acute lymphoblastic leukemia. Onco Targets Ther 10: 1413-1422, 2017.
11. Zhang HL, Bai ZY, Zhang MX and Xi YF: Advances in molecular genetics of acute T lymphoblastic lymphoma/leukemia. Zhonghua Bing Li Xue Za Zhi 49: 870-873, 2020 (In Chinese).
12. Zhang Hong CB: Clinical analysis of 241 cases with multiserosal cavity effusion. J Clin Int Med 20: 644-646, 2003.
13. Losada I, González-Moreno J, Roda N, Ventayol L, Borjas Y, Domínguez FJ, Fernández-Baca V, García-Gasalla M and Payeras A: Polyserositis: A diagnostic challenge. Intern Med J 48: 982-987, 2018.
14. Li Jiao ZY, Qu Yi and Mu Zhi: Evidence-based evaluation of the diagnostic value of adenosine deaminase in tuberculous serosal cavity effusion. Chin J Evidence-Based Med 10: 495-498, 2010.
15. Portell CA and Sweetenham JW: Adult lymphoblastic lymphoma. Cancer J 18: 432-438, 2012.
16. Liu K, Gao Y, Han J, Han X, Shi Y, Liu C and Li J: Diffuse large B-cell lymphoma of the mandible diagnosed by metagenomic sequencing: A case report. Front Med (Lausanne) 8: 752523, 2021.
17. Mohammad NS, Nazli R, Zafar H and Fatima S: Effects of lipid based multiple micronutrients supplement on the birth outcome of underweight pre-eclamptic women: A randomized clinical trial. Pak J Med Sci 38: 219-226, 2022.
18. Wei P, Gao Y, Zhang J, Lin J, Liu H, Chen K, Lin W, Wang X, Wang C and Liu C: Diagnosis of lung squamous cell carcinoma based on metagenomic next-generation sequencing. BMC Pulm Med 22: 108, 2022.
19. Shlien A and Malkin D: Copy number variations and cancer. Genome Med 1: 62, 2009.
20. Taylor AM, Shih J, Ha G, Gao GF, Zhang X, Berger AC, Schumacher SE, Wang C, Hu H, Liu J, *et al*: Genomic and functional approaches to understanding cancer aneuploidy. Cancer Cell 33: 676-689.e3, 2018.

21. Guo Y, Li H, Chen H, Li Z, Ding W, Wang J, Yin Y, Jin L, Sun S, Jing C and Wang H: Metagenomic next-generation sequencing to identify pathogens and cancer in lung biopsy tissue. EBioMedicine 73: 103639, 2021.
22. Zheng D, Zeng L, Gu H and Guan X: Clinical studies of cell chromosomal detection in the diagnosis of malignant multiserosal cavity effusion. Chin J Clinicians (Electronic Edition) 3: 602-607, 2009.
23. Yan L, Sun W, Lu Z and Fan L: Metagenomic next-generation sequencing (mNGS) in cerebrospinal fluid for rapid diagnosis of Tuberculosis meningitis in HIV-negative population. Int J Infect Dis 96: 270-275, 2020.